ELECTROLYTIC SMELTING OF LUNAR ROCK FOR OXYGEN, IRON, AND SILICON

Larry A. Haskin, Russell O. Colson, David J. Lindstrom[1], Robert H. Lewis[2], and Krystyna W. Semkow[3]

Department of Earth and Planetary Sciences and McDonnell Center for the Space Sciences
Washington University
St. Louis MO 63130

Preliminary studies of the electrochemical properties of silicate melts such as those available from heating of lunar mare soils indicate that conductivities are high enough for design of a practical electrolytic cell. The nature and kinetics of the electrode reactions, which involve reduction of Fe^{2+} and Si(IV) and oxidation of silicate anions as the primary, product-forming reactions, are also satisfactory. A survey of the efficiencies for production (amount of product for a given current) of O_2, Fe^0, and Si^0 as functions of potential and of electrolyte composition indicate that conditions can be chosen to yield high production efficiencies. We also conclude that electronic conductivity does not occur to a significant extent. Based on these data, a cell with electrodes of 30 m^2 in area operating between 1 and 5 V with a current between 1.6 and 3.5×10^5 A for a mean power requirement of 0.54 MW and total energy use of ~13 MWhr per 24-hr day would produce 1 tonne of O_2, 0.81 tonne of Fe^0, 0.65 tonne of Si^0 (as Fe^0-Si^0 alloy), and about 3.5 tonnes of silicate melt of altered composition per 24 hr. Adjustable distance between electrodes could offer flexibility with respect to feedstock and power source.

INTRODUCTION

As the breadth of activities in near-Earth space increases, we will need increasing amounts of materials for use there. Because of Earth's substantial gravitational well, the ratio of payload delivered per unit of launch energy is rather low, even for hauling materials to low-Earth orbit (LEO) (300-500 km). The Moon has only one-sixth the gravity of Earth, and a given amount of energy will boost many times as much payload from the surface of the Moon to LEO as from the surface of Earth to LEO. Because the cost of each launch from Earth is high, it is possible that the Moon could be a cheaper source than the Earth for bulky, relatively unspecialized materials for use in space. Comparisons must include the combined costs of mining, smelting, manufacturing, and transporting the nonterrestrial material.

One material we expect to need in increasing quantities in LEO is oxygen, mainly for use as the oxidizer in propellant. We might be able to supply oxygen economically from the Moon for use in LEO. Oxygen is the most abundant element in the lunar regolith, where it occurs in chemical combination with metallic elements (*Haskin and Warren,* 1991). There remains the possibility that water, another potential source of oxygen, will be found at the lunar poles (*Arnold,* 1979; *Lanzerotti and Brown,* 1981), but we ignore that possibility here.

Other bodies with even lower gravity than the Moon are also potential sources of oxygen for use in LEO. However, we cannot at this time estimate accurately the economics of providing oxygen from Phobos, Deimos, or a near-Earth asteroid relative to lunar oxygen or terrestrial oxygen. While we have theoretical reasons to believe that some asteroids and possibly the satellites of Mars may have water bound in their minerals, we have not verified the presence of such water by direct observation. We do not know the natures of the regoliths of these bodies or how to mine them. (We know little enough about how to mine the Moon.) We do not know how much more difficult mining and extraction might be on bodies with nearly zero gravity than on the Moon with its one-sixth gravity. For now, the only extraterrestrial materials that we know enough about to plan in some detail to use are those abundant materials whose chemical and physical characteristics and setting we know, namely, the lunar soils and, at Hadley Rille, mare basalts. We note that there is currently no means to transport mining and extraction apparatus from Earth to either the Moon or the other bodies.

We believe the Moon, because of its proximity and because of our knowledge of its regolith, is the most sensibly accessible source of significant amounts of extraterrestrial material for the near future. Furthermore, it may be feasible to extract hydrogen for use as a propellant, so both fuel and oxidizer can be furnished for use on the Moon and in LEO (*Haskin,* 1991). Although the Moon apparently accreted very low initial concentrations of volatile materials such as water and carbon compounds, and even if it does not have abundant polar water *per se,* its soils contain large quantities (albeit at very low concentrations) of hydrogen, carbon, nitrogen, and noble gases of solar wind origin.

The purpose of this paper is to add to our understanding of how lunar material might be used as a source of oxygen. In particular, we report results of experiments on electrolysis as a means of producing oxygen, metals, and silicates of altered composition. Electrolysis is well suited to lunar conditions in the sense that it does not require an extensive set of companion processes to produce specialized reagents or materials present in Earth's environment but absent on the Moon. It does not require a continuous supply of materials from Earth. It does not require water for use as a cheap extracting agent or cooling agent, or air to serve as an oxidizing agent or cooling agent. It does not require terrestrial reagents such as wood, coal, or even limestone, nor does it require prepared chemicals to serve as reagents or

[1] Now at Mail Code SN2, NASA Johnson Space Center, Houston TX 77058
[2] Now at GE Astro Space Division, P.O. Box 800, Princeton NJ 08543-0800
[3] Now at Department T40, IBM Corp., Box 8003, 1701 North Street, Endicott NY 13760

feedstocks. It will not be compromised by the Moon's strong vacuum and should not be strongly affected by its low gravity. It requires only heat, electrical power, and a suitable electrolytic cell. It can use a relatively unspecialized feedstock such as finely pulverized lunar soil, and can make use of available sunlight for heat and electrical power.

We have begun laboratory bench-scale testing to determine whether electrolysis of molten lunar soil or rock should be further considered as a viable process for smelting on the Moon to yield oxygen gas and iron and silicon metals. Our approach is to understand the fundamental electrochemcial properties of silicate melts and to estimate from them the parameters of an electrolytic separation system. In particular, we have adapted well understood procedures for voltammetry and chronopotentiometry and applied them to silicate melts at high temperatures, and have identified the competing anodic and cathodic reactions (*Semkow et al,* 1982; *Semkow and Haskin,* 1985). We have measured conductivities of simulated lunar silicates. We have made a preliminary determination of the efficiency for the reduction of Fe^{2+} and Si(IV) to metal. We have evaluated the possibility that transition metal silicates conduct electronically. We have measured efficiencies for production of O_2 as functions of the partial pressure of oxygen surrounding the melt (fO_2), electrode potential, and melt composition. Finally, we have made first-cut estimates of the operating parameters for a producing electrolytic cell.

ELECTRODE REACTIONS

While previous studies (*Oppenheim,* 1968; *Kesterke,* 1971; *Lindstrom and Haskin,* 1979) showed clearly that oxygen gas and iron metal are products of the electrolysis of silicate melts with compositions similar to those of the basaltic lavas that we find in the lunar maria, they did not include investigations of the nature of the electrode reactions or their kinetics. This is a difficult problem if one begins with a melt as complex as a basaltic lava, so we have done many of our fundamental studies in molten diopside ($CaMgSi_2O_6$) to which FeO has been added. To a very rough approximation, but one adequate for our purposes, the bulk composition of basaltic magmas corresponds to half diopside and half plagioclase feldspar ($CaAl_2Si_2O_8$). Our initial results for mixtures of diopside and feldspar show that the types of reactions are the same as, or very similar to, those in diopside. We conclude that our studies pertaining to diopsidic melt are applicable to basaltic melts as well.

Cathodic Reactions

There are two major metal-producing cathodic reactions; one is the following

$$\text{Cathodic: } Fe^{2+} + 2e^- = Fe^0 \qquad (1)$$

Nickel, cobalt, and zinc existing as Ni^{2+}, Co^{2+}, and Zn^{2+} in diopsidic melt each show a simple, reversible, two-electron transfer reduction (*Semkow et al.,* 1982). Our preliminary studies of iron (*Rizzo,* 1976), which is present partly as Fe^{2+} and partly as Fe^{3+}, suggest that the reduction of Fe^{2+} is also a simple reversible process, as represented by equation (1). However, these studies involved metallic-state atoms dissolved in the silicate melt. The reduction of the cations to solid or liquid metal in a separate phase would occur at potentials a few hundred millivolts more negative than observed in the studies of Semkow et al. and Rizzo. (The exact difference depends on the activities of the oxidized and reduced species in the melts.)

The second major metal-forming cathodic reaction is the reduction of Si(IV) [equation (2)]. The silicon, depending on conditions, will be alloyed to varying extents with iron.

$$\text{Cathodic: } Si(IV) + 4e^- = Si^0 \qquad (2)$$

A competing cathodic reaction is reduction of Fe^{3+} that is present in the feedstock or produced at the anode [equation (3)]. This reaction is important when the concentration of Fe^{2+} exceeds a few percent (discussed in detail below).

$$\text{Cathodic: } Fe^{3+} + e^- = Fe^{2+} \qquad (3)$$

Another competing cathodic reaction, the reduction of O_2 [equation (4)], can become important at oxygen fugacities above 10^{-4}. Since the cell produces an atmosphere of oxygen above it, and since oxygen is slightly soluble in silicate melts (Henry's Law constant ~0.023 moles/liter/atmosphere in diopside at 1450°C; *Semkow and Haskin,* 1985), some oxygen is reduced at the cathode as in equation (4).

$$\text{Cathodic: } O_2 + 4e^- = 2O^{2-} \qquad (4)$$

These reactions [equations (3) and (4)] compete with the reduction of Fe^{2+} and Si(IV) for electrons and can significantly reduce the efficiency of metal production.

Reductions of minor and trace cations such as Cr^{3+}, Cr^{2+}, Ti^{4+}, Ti^{3+}, and Mn^{2+} may also occur, but we have not yet determined the conditions for this.

Anodic Reactions

Initially, we considered the principal anodic reaction to be the following (*Lindstrom and Haskin,* 1979)

$$\text{Anodic: } 2O^{2-} = O_2 + 4e^- \qquad (5)$$

However, the reaction that produces oxygen at the anode is more complicated than equation (5) implies. Concentrations of oxide ion are buffered at very low levels in these melts, (approximately 10^{-5} mole/liter; *Semkow and Haskin,* 1985). In principle, the buffering reaction should ensure a steady supply of O^{2-}, according to the equilibrium represented by equation (6). However, the equilibrium concentration of O^{2-} is low, and the rate of depolymerization to yield O^{2-} by reaction of a pair of nonbridging oxygens is slow. Thus, reaction (5) is unimportant to practical electrolysis.

$$\text{Melt: } 2(SiO\text{-}) = (Si\text{-}O\text{-}Si) + O^{2-} \qquad (6)$$

In equation (6), (SiO-) represents a "nonbridging" oxygen attached to a silicon that is part of a polymer chain, and (Si-O-Si) represents a "bridging" oxygen attached to two Si atoms and part of a polymer chain. Bridging oxygens are presumed to form covalent bonds between two Si atoms, and nonbridging oxygens are presumed to bond covalently with one Si and more or less ionically with some other cation such as Fe^{2+} or Mg^{2+}. Independent polymer chains become linked together, or a single, long chain becomes linked to itself, when reaction (6) takes place.

The important anode reaction thus involves the breakdown of silicate anion, resulting in an increase in the extent of polymerization of the melt, as shown in equation (7). The rate of this reaction is fast.

$$\text{Anodic: } 4(\text{SiO-}) = 2(\text{Si-O-Si}) + O_2 + 4e^- \quad (7)$$

In melts with high concentrations of Fe^{2+}, the competing reaction occurs at the anode [equation (8)]

$$\text{Anodic: } Fe^{2+} = Fe^{3+} + e^- \quad (8)$$

Oxidations of Ti^{3+} and Cr^{2+} can also be expected when those species are present.

CONSTRAINTS ON CELL DESIGN

To calculate how much power is required to extract a given amount of product, we must know the resistance of the electrolytic cell and the efficiency at which O_2, Fe^0, and Si^0 are produced. These two parameters are functions of the potential imposed between the electrodes, the composition of the silicate used as feedstock, the oxygen fugacity, and the cell configuration (including surface areas of the electrodes and distance between the electrodes). By measuring melt conductivities and production efficiencies as functions of composition and potential, it becomes possible to demonstrate that a cell of reasonable and robust dimensions can be designed. Furthermore, by estimating the purity of the products and determining the effect of the product on various possible electrodes (most of which effects can be gleaned from the metallurgical literature), it is possible to put constraints on the type of materials that could survive as electrodes.

Silicate Conductivity

Resistance of the cell is a function of electrode surface area, distance between electrodes, and conductivity of the chosen feedstock. The power needed to drive the electrolysis increases as resistance increases. Thus, the limitations on the power that can be delivered, the size and weight of the electrolysis cell, and the distance the electrodes must be apart to remain robust during transport and use constrain the conductivity that the melt must have in order to conduct current adequately. Therefore, we have determined the conductivities in the temperature range 1420-1550°C of molten silicates with compositions similar to those of molten lunar rocks and soils. These determinations, like most of our other electrochemical measurements, were made on small samples (80-100 mg each) of silicate melts suspended in horizontal loops of Pt wire and held there by surface tension (see *Lindstrom and Haskin,* 1979). For conductivity measurements, a second Pt wire passed through each melt at right angles to the plane of the wire loop. The potential drop between the electrodes and across a series reference resistor provided a measurement of potential and resistance. Potentials between the electrodes of a few millivolts were used.

The values lie in the range 0.08-40 $ohms^{-1}cm^{-1}$ and are strongly dependent on melt composition, as shown in Figs. 1 and 2 (at high alternating current frequencies). These values appear adequate for robust cell design, as discussed in more detail below. Compositions of melts, made up from high-purity oxide powders, are given in Table 1. A systematic variation in conductivity with

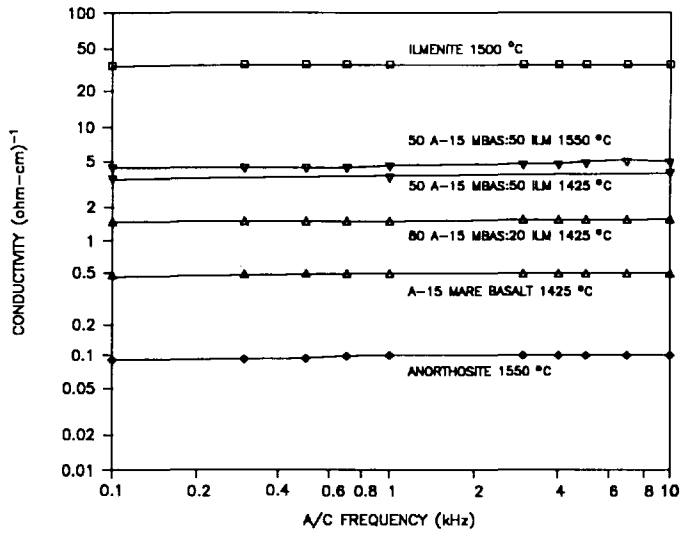

Fig. 1. Conductivities of melts of simulated Apollo 15 mare basalt, simulated anorthosite rock, ilmenite, and mixtures of simulated Apollo 15 mare basalt and ilmenite are shown as a function of alternating current frequency. Note that conductivity increases as the state of polymerization of the silicate anions (highest in anorthosite, absent in ilmenite) decreases. Note also the increase in conductivity with temperature for 50:50 mixtures of simulated mare basalt and ilmenite. Values determined in our laboratory (*Lewis,* 1985), but multiplied by 1.43 to correct for an erroneous value of the cell constant used in that work).

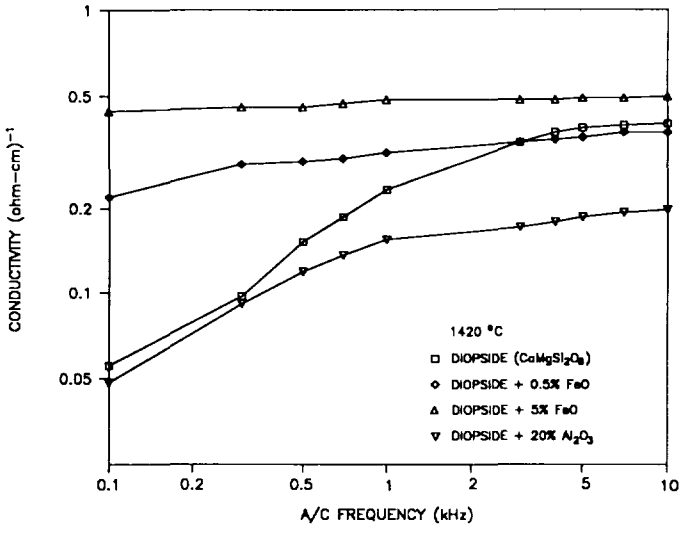

Fig. 2. Conductivities of molten diopside ($CaMgSi_2O_6$) and of diopside mixed with FeO, which increases the concentration of mobile cations and decreases the extent of silicate polymerization, and with alumina (Al_2O_3), which increases the extent of anion polymerization and lowers the conductivity. Note that the conductivities of diopside and of diopside mixed with alumina decrease with decreasing alternating current frequency, as expected for polarized melts that serve as dielectrics. In contrast, the conductivity of melts containing Fe^{2+} does not change appreciably with decreasing frequency, owing to reduction of Fe^{2+} at the cathode and oxidation of Fe^{2+} at the anode.

TABLE 1. Compositions of melts used for conductivity studies (given as oxide wt%).

	Apollo 15 Mare Basalt	Anorthosite	Ilmenite	Diopside
SiO_2	45.64	43.67		55.49
TiO_2	2.48	0.13	52.65	
Al_2O_3	9.04	33.1		
FeO	22.75	1.92	47.35	
MgO	9.9	2.69		18.61
CaO	10.18	18.41		25.9
Na_2O		0.08		

composition is observed and is shown in Fig. 3. The coefficients of the compositional parameters plotted along the abscissa were determined by linear regression.

The theoretically expected variation of conductivity with composition at constant temperature can be expressed by equation (9).

$$\text{Conductivity} \propto \Sigma X_i D_i Z_i^2 \qquad (9)$$

In equation (9), X_i is the molar concentration of i, D_i the diffusivity of i, and Z_i the charge of i (*Rieger,* 1987, p. 160). This expression is similar to our empirical relationship of Fig. 3, and the values of our regression coeffficients should be related to $D_iZ^2_i$. Estimating values for D_i from the work by *Hendersen et al.* (1961) and Fig. 8 of *Henderson et al.* (1985), we have estimated values for $D_iZ^2_i$ and compare them to our regression coefficients in Fig. 4. The correlation supports the use of our empirical relationship to describe the variation of conductivity with composition.

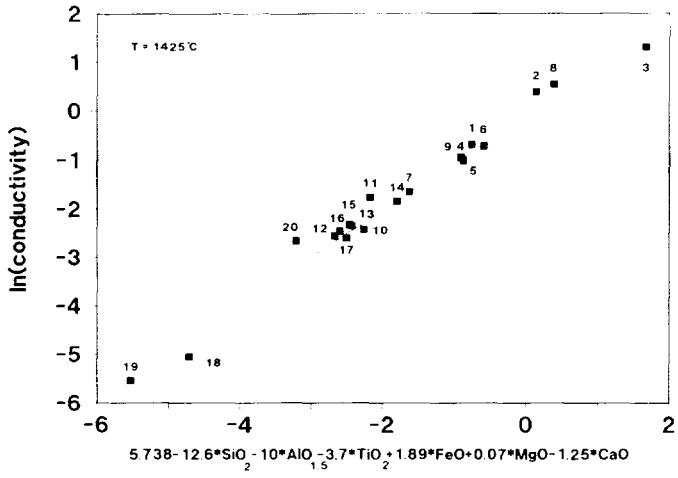

Fig. 3. Dependence of conductivity at 1425°C on melt composition. Symbols for oxides stand for mole fraction in the empirical equation used to calculate the values along the abscissa; values of the coefficients were determined by linear regression. Except where noted, data are from *Lewis* (1985). $R^2 = 0.99$. Compositions are: 1 = Apollo 15 basalt (A15); 2 = A15 + 20% Ilm; 3 = A15 + 50% Ilm; 4 = Di; 5 = Di + 0.5% FeO; 6 = Di + 5% FeO; 7 = Di + 20% Al_2O_3; 8 = Hd; 9 = Di + 0.5% NiO; 10 = Di + 50% An; 11 = A15 + 20% Ilm (FeO free); 12 = A15 (FeO free); 13 = Anorthositic gabbro; 14 = Wo + 20% Al_2O_3; 15 = Wo + 50% An; 16 = Wo + 40% Al_2O_3; 17 = Ge + 50% An; 18 = An + 20% SiO_2; 19 = An + 35% SiO_2; 20 = Anorthosite (from *du Fresne and Schroeder,* 1983).

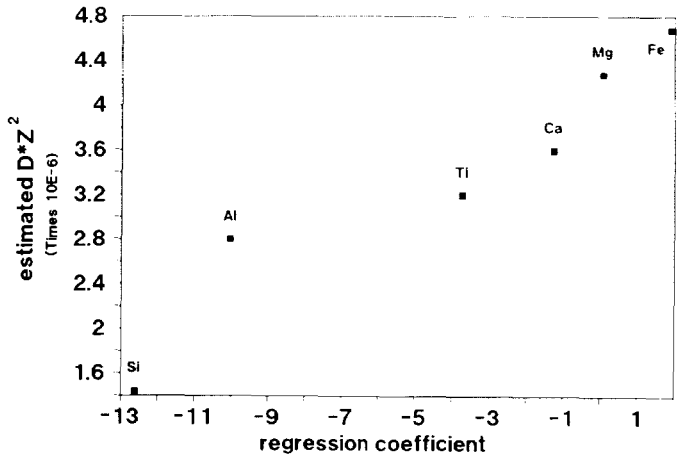

Fig. 4. Comparison between the coefficients determined by linear regression in the plot of Fig. 3 and estimates of electric mobilities (diffusivity times charge squared) of selected cations. Diffusivities for Ti^{4+}, Mg^{2+}, and Fe^{2+} were not available and are approximated roughly from Fig. 8 of *Hendersen et al.* (1985). The regression coefficients correlate well with expected electric mobilities suggesting that Fe^{2+} does not cause an unexpected increase in conductivity, such as might result from electronic conduction.

Efficiencies of Production

We consider two things pertaining to the efficiency of production of O_2 and metals. First, there was reason to suspect that significant electronic conduction might occur (semiconduction by electrons or holes). Electronic conduction in silicate melts has been previously proposed (e.g., *du Fresne and Schroeder,* 1983; *Mackenzie,* 1962; and *Simnad et al.,* 1954). The initial suggestion of this, made by *Simnad et al.* (1954), was based on an observed decrease in efficiency of oxygen production with increasing Fe concentrations in a series of melts consisting of FeO and SiO_2 in different proportions. Other evidence includes the absence of any observed change in conductivity during fusion of FeO, which is known to be semiconducting as a solid (*Mackenzie,* 1962). If there were a large component of electronic conduction, our electrolytic cell would be shorted out and efficiencies would be low.

Second, efficiencies for a given product are affected by reactions such as the reduction of Fe^{3+} to Fe^{2+} at the cathode and the oxidation of Fe^{2+} at the anode, which in turn depend on the composition of the melt. The composition of the melt also affects the composition of the metal produced through the proportions of Si(IV) and Fe^{2+} reduced at the cathode.

Electronic conductivity in iron-bearing silicates? The near constancy of conductivity with alternating current frequency seen in Fig. 1 does not at first appear to be consistent with current flow by simple ionic conductivity in the melt. If a direct potential is emplaced across two electrodes in an ionic melt, ions of positive charge migrate toward the cathode and those with negative charge away from it, and vice versa for the anode. This process continues only momentarily, until the electric field produced by the external potential is matched by an equal potential of opposite polarity resulting from partial separation of charges in the melt, a condition known as "polarization" of the melt. When this occurs, no more net separation of charge can

occur in the melt, and the current falls to zero. Thus, the melt serves as a dielectric and the device behaves as a capacitor, unless potentials are high enough to reduce or oxidize ions in the melt, in which case the discharge of ions at the two electrodes offsets the polarization.

At high alternating current frequencies, there is insufficient time for ions to migrate far enough in one direction to polarize the melt. Thus, potential differences between electrodes induce migration of ions within the melt, resulting in flow of current. As the frequency of the alternating current is decreased, partial polarization takes place, decreasing the average strength of the electric field over each cycle, and thus decreasing the mean value of the current per cycle. Finally, at the lowest of frequencies (direct current), the melt polarizes completely and there is no current beyond the initial polarizing current.

The expected decrease of conductivity with decreasing alternating current frequency is readily seen for molten diopside, $CaMgSi_2O_6$, and for molten mixtures of diopside and alumina (Fig. 2). Addition of even a small amount of FeO to the melt drastically increases the conductivity of diopside at low alternating current frequencies. This effect has been interpreted by some investigators as suggesting electronic conductivity in transition metal-bearing silicates. The same effect is seen when CoO or NiO are added to the melts.

Efficient electrolysis requires that passage of current between melt and electrode be by discharge of ions at the electrode, not by direct transfer of mobile electrons and holes that can move through the melt. Thus, we have done experiments to determine whether an appreciable fraction of the conductivity in iron-bearing silicate melts is by strictly electronic means. The evidence suggests that there is no appreciable electronic conductivity. The reasons are as follows:

1. The increase in conductivity per mole of divalent ion added is nearly the same for the transitional elements Fe^{2+}, Co^{2+}, Ni^{2+}, and Zn^{2+} as for the nontransitional elements Mg^{2+} and Ca^{2+}. It corresponds closely to the increase expected per mole from increasing the concentrations of mobile divalent cations relative to sluggish, highly polymerized silicate anions. The relative effects of different cations on conductivity can be seen from Figs. 3 and 4. The increase in conductivity from adding Fe^{2+} is close to that expected based on Fe^{2+} diffusivity, suggesting that the melt structure does not change in a fundamental way to enable a new form of conductivity when the transitional elements are added.

2. The conductivities of diopside and diopside plus alumina (Fig. 2) are low compared with that of diopside plus small concentrations of added FeO. If the difference reflects electronic conduction by iron-bearing melts, the bulk of the conduction in those melts should be electronic. However, preliminary measurement of the efficiency of electrolysis for reduction of Fe^{2+} to Fe^0 in our test system (≥60%; *Lindstrom et al.,* 1986) shows that the bulk of the conductivity must be ionic. In these small samples, we expect that at least some Fe^{3+} and O_2 find their way to the cathode through convection, requiring that some additional oxidation and reduction take place. This leaves little, if any, current to be accounted for by electronic transport.

3. Addition of the transition metal ion Zn^{2+} raises the conductivity at high frequencies to an extent commensurate on a per mole basis to that of the other divalent ions, but does not maintain the level of conductivity at low frequencies that Fe^{2+}, Co^{2+}, and Ni^{2+} do. Thus, an ion that can be reduced almost as easily as Fe^{2+}, Co^{2+}, and Ni^{2+} does not show the effect.

This suggests that the ability of Fe^{2+}, Co^{2+}, and Ni^{2+} to be reduced to the metallic state or oxidized to the 3+ state accounts for the relatively high conductivities at low alternating current frequencies. The tendency for Fe^{2+} to oxidize to Fe^{3+} competes with oxygen production, and this presumably explains the observations of *Simnad et al.* (1954). In systems containing those ions, whatever polarity the electrodes have, ions can be discharged at both electrodes. This cannot occur when only Mg^{2+} or Ca^{2+} is present, because their reduction potentials exceed the breakdown potential for polymeric silicate and their oxidation potentials would be extremely high. It cannot occur when Zn^{2+} is added because, although Zn^{2+} reduces readily at the cathode, its oxidation potential is so high that no complementary anodic reaction can occur.

Given this mechanism for maintenance of the high conductivity, we can describe the resistance of our electrolytic cell, at least approximately, in terms of the circuit diagram shown in Fig. 5. The resistance R_i represents the resistance of the melt to ionic conduction (related to the intrinsic mobilities of the ions in the melt); R_c represents the resistance associated with reduction at the cathode and is related to the reduction potentials of Fe^{2+} and Si(IV) and their concentrations in the melt; R_a represents the resistance associated with oxidation at the anode and is related to the oxidation potential of the silicate anions; C represents the electrode-melt capacitance.

Competing reactions at the cathode. As discussed above, several competing reactions can occur at the cathode along with the reduction of Fe^{2+}. We have estimated the dependence of the efficiency of Fe metal production on potential and on electrolyte composition by a combination of theoretical treatment and experiment. Experiments were designed to determine the difference between "background" current flow (related to reductions other than Fe^{2+}) and total current. This was done by measuring current as a function of potential (in this case, cathodic potential relative to the potential of the bulk electrolyte) for both a silicate melt containing Fe^{2+} and a silicate melt in which a molar-equivalent amount of electroinactive Mg^{2+} had been substituted for Fe^{2+}.

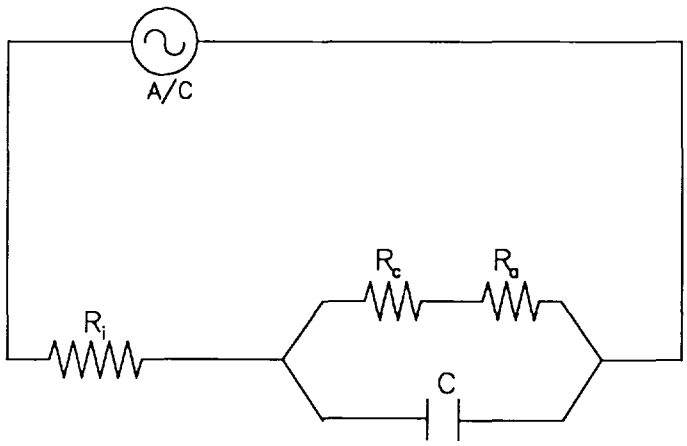

Fig. 5. Circuit diagram model to represent the electrical properties of the molten silicates. The overall resistance of the cell to alternating current stems from the combined resistance of ionic conductivity (R_i), the threshold potentials for the cathodic and anodic redox reactions (R_c and R_a), and the charging current capacitance of the cell as it polarizes (C).

Figure 6 shows cathodic current as a function of electrode potential for several compositions. The "background" current is for a composition in which Mg^{2+} has been substituted for Fe^{2+}. This current is related primarily to the reduction of Si(IV). If we assume that no current is lost to electronic conduction (as discussed above), then the figure gives a rough estimate of the relative amounts of the total current that can be attributed to the Fe^{2+} and Si(IV) reductions at various potentials and Fe^{2+} concentrations. However, for these compositions and potentials, much of the reduced Fe^0 is dissolved in the melt or in the Pt electrodes and does not exist as precipitated, pure metallic Fe.

Threshold potentials for the precipitation of pure metallic Fe were calculated from the data presented by *Grove* (1981) and are plotted as a function of cation mole percent of Fe^{2+} in Fig. 7. Figure 7 indicates that, in the range of potentials 0 to -250 mV, pure metallic Fe can only be precipitated at concentrations >11 mol% Fe^{2+} (or FeO). Comparison with Fig. 6 indicates that at those potentials and concentrations, the amount of Fe^{2+} reduced will be very large compared to the amount of Si(IV) reduced.

We conclude that at high Fe^{2+} concentrations (>20% FeO) and low potentials (e.g., 0 to -0.4 V at $fO_2 = 10^{-8}$), the cathode product is primarily Fe^0. At lower Fe^{2+} concentrations (<5% FeO) and higher potentials (e.g., >0.4 V at $fO_2 = 10^{-8}$), the cathodic product is primarily Si^0.

Competing reactions at the anode. Efficiency of O_2 production [defined as moles of O_2 produced/(moles of electrons passed through the melt/4)] is calculated from the amount of O_2 produced and the measured total current flow in an electrolysis experiment. The amount of O_2 produced is determined from the difference in sample weight before and after the experiment.

We find that the primary reaction competing with oxygen formation at the anode is the oxidation of Fe^{2+}. This oxidation controls the dependence of oxygen production efficiency on electrode potential, oxygen fugacity, and electrolyte composition. Oxygen production efficiency decreases as Fe^{2+} concentration increases. Fe^{2+} concentration increases both as the melt becomes richer in iron and as oxygen fugacity decreases. If we assume that

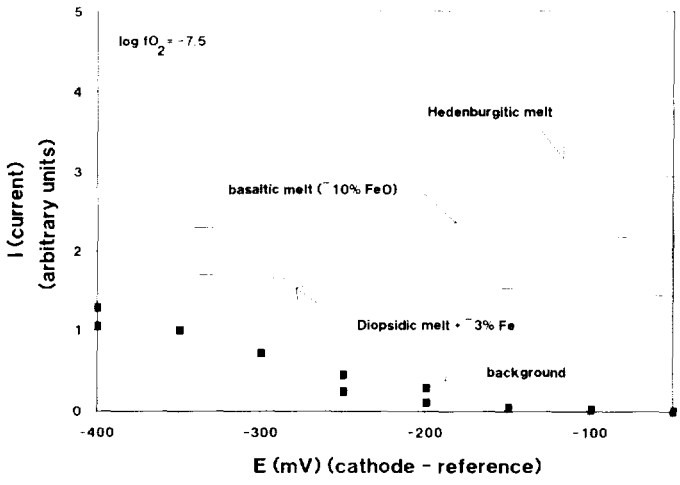

Fig. 6. Proportions of current (as a function of cathode potential) that can be attributed to Si(IV) reduction (background) and Fe^{2+} reduction (other curves minus background) for melts of several Fe^{2+}concentrations. Note that the proportion from Fe^{2+} reduction increases as Fe^{2+} concentration increases and decreases with increasing potential.

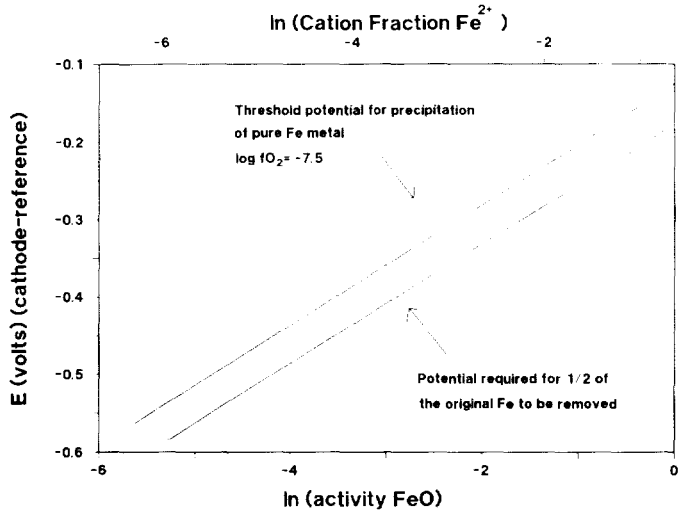

Fig. 7. Potential required to reduce Fe^{2+} to Fe^0 in the presence of pure metallic Fe, estimated from the data of *Grove* (1981). Activity of FeO is defined in *Grove* (1981), $AFeO = XFe^{2+}/(XFe^{2+} + XMg^{2+} + XCa^{2+} + XAl^{3+} - XK^{+} - XNa^{+})$ where X denotes cation mole fraction. An approximate conversion to a standard state of activity of Fe^{2+} defined as a simple cation fraction is shown along the top of the figure. Note that these potentials are somewhat more negative than the lowest potentials in Fig. 6, in which significant current flow is observed, reflecting the dissolution of the Fe^0 of the experiments of Fig. 6 in the melt and in the Pt electrodes.

all the current is related to oxidation of either oxygen ions or Fe^{2+}, we can estimate the relative proportions of the current attributable to each oxidation by equation (10), where $\%Fe^{2+}$ is the percent of the current attributed to the oxidation of Fe^{2+}, $\%O_2$ is the percent of the current producing oxygen, $X(Fe^{2+})$ is the cation mole fraction of Fe^{2+}, and $X(O^{2-})$ is the mole fraction of oxidizable oxygen (which we assume is constant).

$$\%Fe^{2+}/\%O_2 = X(Fe^{2+})/X(O^{2-}) \qquad (10)$$

If we further normalize the concentrations of these electoractive species such that $\%Fe^{2+} + \%O_2 = 100\%$, equation (10) can be modified to yield equation (11).

$$\%O_2/(100-\%O_2) = X(O^{2-})/X(Fe^{2+}) \qquad (11)$$

This relationship adequately describes the observed dependence of O_2 efficiency on composition and oxygen fugacity, as is shown in Fig. 8. The dependence of $\%O_2$ on total Fe (rather than ferrous Fe) [equation (13)] can be obtained from the expression for equilibrium [equations (12) and (11)].

$$X_{FeO} = X_{FeO1.5}/(fO_2^{1/4}e^{-\Delta G/RT}) \qquad (12)$$

In equation (12), ΔG is the Gibbs Free Energy for the oxidation of FeO to $FeO_{1.5}$. X_{FeO} (or Fe^{2+}; we express the concentrations for all cations as cation mole fractions) can be expressed as $X_{totalFe}/fO_2^{1/4}e^{-\Delta G/RT} + 1)$ and substituted into equation (11) to give equation (13).

$$\%O_2/(100-\%O_2) = XO^{2-}(fO_2e^{-\Delta G/RT} + 1)/X_{totalFe} \qquad (13)$$

ΔG is a function of composition and temperature, and estimates of its value can be made from studies such as that of *Sack et al.* (1980).

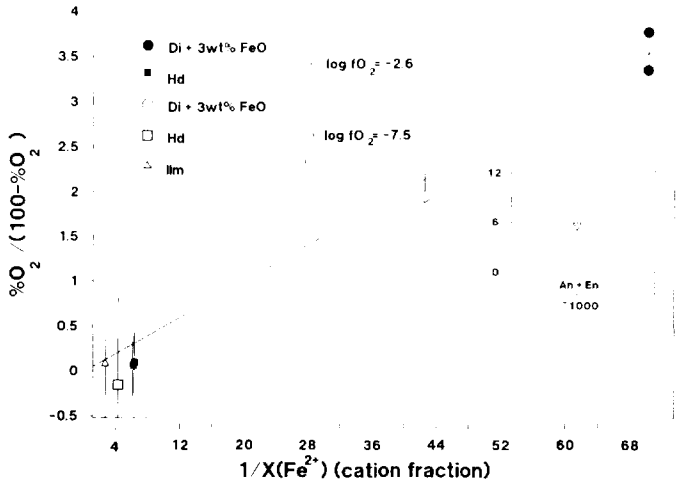

Fig. 8. Dependence of O_2 production efficiency on Fe^{2+} concentration in the melt. The mole fraction of Fe^{2+} as a function of fO_2 is calculated from the concentration of total iron and the reduction potential for Fe^{3+}.

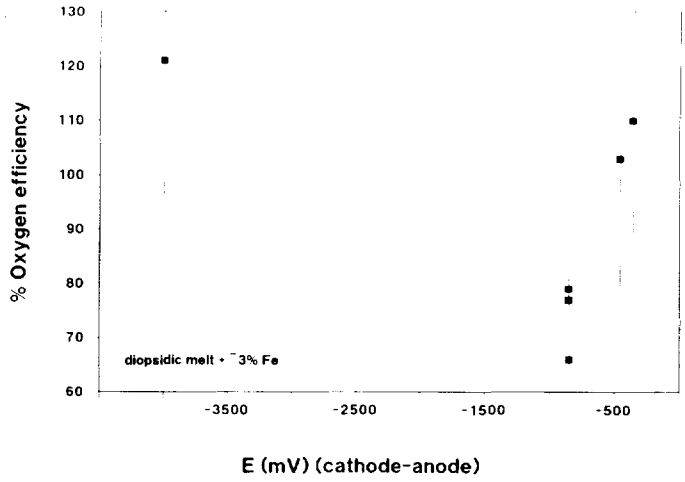

Fig. 9. Dependence of O_2 production efficiency on potential. The lowest efficiences are near the Fe^{3+} reduction potential. Bars show estimates of uncertainty.

The dependence of O_2 efficiency on cell potential (Fig. 9) can also be related to the oxidation of Fe^{2+}. The low point in the oxygen efficiency curve is near the reduction potential for Fe^{3+}. (Based on Fe^{3+} reduction potentials, we estimate about 35-65% of the Fe^{2+} is oxidized at these potentials.) At potentials less negative than the reduction potential for Fe^{3+}, only a small fraction of the Fe^{2+} is oxidized to Fe^{3+} (we estimate 5-10%). At higher potentials the amount of Fe^{2+} that is oxidized is small compared to the amount of oxygen because oxygen is so much more abundant in the melt than Fe^{2+}. However, for melts with high Fe^{2+} concentrations, increasing the potential does not significantly increase the efficiency of O_2 production. We conclude that high efficiencies for O_2 production require low Fe^{2+} concentrations, high oxygen fugacity (from the point of view of high Fe^{3+}/Fe^{2+}, but not from the point of view of the competing cathode reduction of O_2), and high potentials. These conditions are the opposite of those required for high Fe^0 production efficiencies.

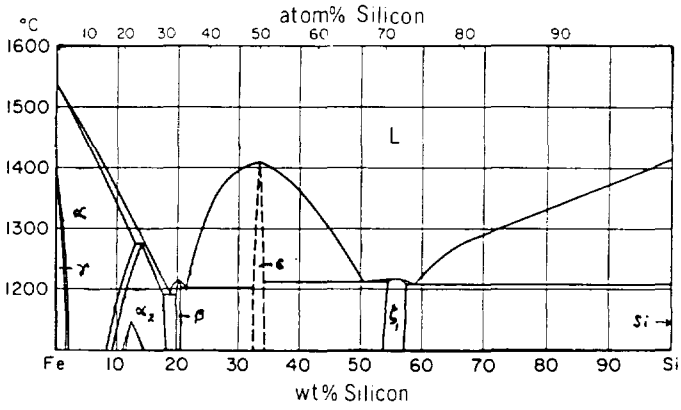

Fig. 10. Silicon-iron binary phase diagram, adapted from *Hultgren et al.* (1973).

Electrode Materials

Several considerations must be made in choosing a material for the cathode. First, the cathode must be inert to or in equilibrium with the cathodic product. The cathode must either be solid itself or it must be contained within a solid that is inert to or in equilibrium with the cathode material, the cathode product, and the silicate melt. Because a solid product may short out the cell by forming dendrites that bridge between electrodes, it is also desirable that the cathode material have a melting point higher than that of the cathodic product. Because the cathodic product will be mostly Fe^0 and Si^0 (minor amounts of Mn^0, Ti^0, and Cr^0 being ignored here), the Si-Fe phase diagram (Fig. 10) is one key to the composition of the cathode.

Basically, three types of Si or Si-Fe electrodes can be used, each one stable relative to different compositions of Si^0-Fe^0 melt. These are pure Si^0 (stable relative to a molten Si-Fe alloy between 0 and about 40 wt% Fe), Fe(67 wt%)-Si alloy (stable relative to a molten Si-Fe alloy between about 50 and 78 wt% Fe), and solid solutions between about 87% and 100% Fe^0 (stable relative to a melt that is only slightly more Si^0-rich than the solid electrode). For an electrolysis aimed at high oxygen production efficiency (therefore having low Fe^{2+} concentrations in the electrolyte with a high Si/Fe ratio in the cathodic product), a Si^0 electrode may be the one of choice despite the high resistivity of Si^0. For electrolysis aimed at Fe^0 production, the Fe-rich alloy electrode may be the one of choice. At high temperatures (e.g., >1200°C), the specific conductivities of these proposed electrode materials are high enough to serve in a practical cell (Fe: *Weast*, 1982; Si: *Pearson and Bardeen*, 1949).

An alternative approach may be applicable if nearly pure Fe^0 is precipitated at the cathode. It is an Fe^0 cathode that also serves as the container and is dynamically cooled such that its outer portions are solid and its inner portions are molten.

A third approach is adapted from one formerly used in the commercial production of Fe-Si alloys. In that process, heat was provided by electrodes positioned near the middle of an electric furnace. The iron silicate feedstock melted in the middle of the furnace but remained chilled against the container walls. The chilled margin served as insulation protecting the container from the reactive silicate melt and the Fe-Si alloy product (*Greiner*, 1933, p. 17).

For the anode, we suggest Pt, possibly in the form of a screen to aid the escape of oxygen bubbles. Silicate melts are extremely corrosive, and few materials can retain their integrity when subjected to them. In preliminary studies (*Semkow and Haskin,* 1986) we investigated the oxidization of Pt as a function of electrode potential and time. In an air atmosphere at 1300° to 1500°C, formation of oxides was the most rapid when the potential of the Pt anode was about 0.2 V positive relative to a separate Pt reference electrode in the same melt. The electrodic oxidation was complex and only a portion of it appeared to be reversible. Nevertheless, during a 5-hr electrolysis of 10 g of molten, iron-rich basalt simulant at a current density of 2.5 A/cm^2 at 1560°C, during which vigorous production of oxygen bubbles was observed, little if any Pt was lost from the anode, a Pt wire of 0.083-cm diameter. Furthermore, efficiencies of as much as 85% for production of O_2 indicate that little of the oxygen reacts with the Pt of the electrode. We surmise that the interior of the electrode may be protected by an outer layer of oxide, and that the rate of evolution of oxygen gas may be in a steady state equilibrium set by the rates of formation and thermal decomposition of oxide in the layer.

EXAMPLE CELL PARAMETERS

Our purpose in this section is to demonstrate that, given our measured conductivities and production efficiencies, an electrolytic cell of reasonable dimensions and production volume can be designed. The variables whose values determine the necessary size and power requirements for the cell include the current necessary to provide oxygen at the desired rate (which must take into account the efficiencies of production), the required energy for the reduction and oxidation processes (including the energy to reduce the oxides and any overpotential required to overcome kinetic problems), and the energy lost to resistance heating of the melt (related to the electrode surface area, the distance between the electrodes, and the melt conductivity).

Some of these variables are constrained by the demands of reasonable cell construction. We select an electrode separation distance >0.5 cm to make sure that the cell will be physically robust. Somewhat arbitrarily, we have constrained the anode and cathode surface areas each to be less than 30 m^2. Some 200 m^2 of electrode surface area can be fit into 1 m^3 volume if 1 m^2, two-sided electrodes are each 1 cm apart. The power should be kept as low as feasible to keep costs low and must not cause runaway heating of the melt. We also choose a production rate for O_2 of 1 tonne per 24 hr. With these constraints in mind, the effect of conductivity and O_2 production efficiency on power requirements are seen in Figs. 11 and 12.

In these figures, the potential required to reduce Fe^{2+} and Si(IV) is taken to be 1.6 V. This potential is considerably greater than that necessary to reduce Fe^{2+} and is sufficient to reduce Si(IV). For conductivities above about 0.4 ohm^{-1}cm^{-1}, efficiencies >0.85 (or 85%), and electrode surface areas >20 m^2, the power required quickly approaches the theoretical minimum value of 0.224 MW. These are encouraging results but, as demonstrated above, efficiency of oxygen production is favored by low Fe^{2+} concentrations in the melts. The effect of this is seen in Fig. 13, which illustrates power requirements for several different compositions with different O_2 efficiencies and conductivities.

As seen from the figure, the power requirement to electrolyze the high-Fe compositions is high, in the range 24-48 MWhr/tonne O_2. This limits us to using either a relatively specialized lunar material such as dunite, which has high concentrations of Mg^{2+} and thus good conductivity and which also has a low concentration of Fe^{2+}, or using a more common material such as magnesian norite or anorthositic norite, which have lower conductivities. Dunite is not known to be as readily available (e.g., in soil form) as materials of more noritic or basaltic compositions, and its high liquidus temperatures make it harder to work with (its liquidus temperatures exceed the melting temperatures of the proposed Si electrodes and container). However, as will be shown below, basaltic and noritic materials work well because their concentrations of Fe^{2+} and Si(IV) are lowered during the progress of electrolysis, increasing the efficiency and conductivity of the melt.

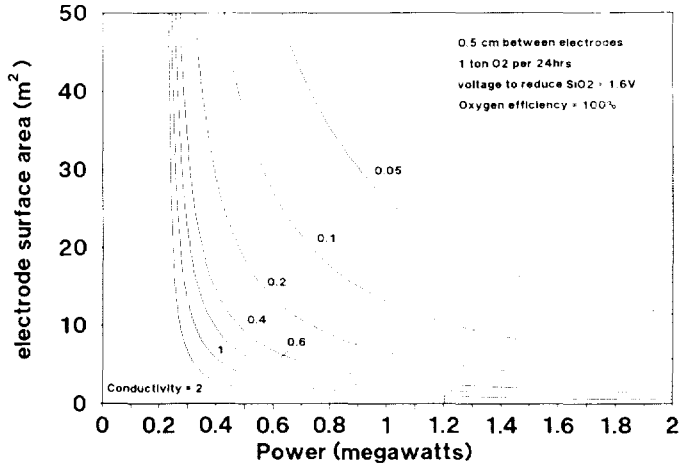

Fig. 11. Effect of electrode surface area and melt conductivity (in ohm^{-1}cm^{-1}) on power required to produce 1 tonne O_2 per 24 hr when the oxygen production efficiency is 100% and the distance between electrodes is 0.5 cm. The potential required to overcome kinetic problems and reduce SiO_2 is taken to be 1.6 V. The energy (in MWhr) to produce 1 tonne of O_2 can be derived from the figure by multiplying the power by 24.

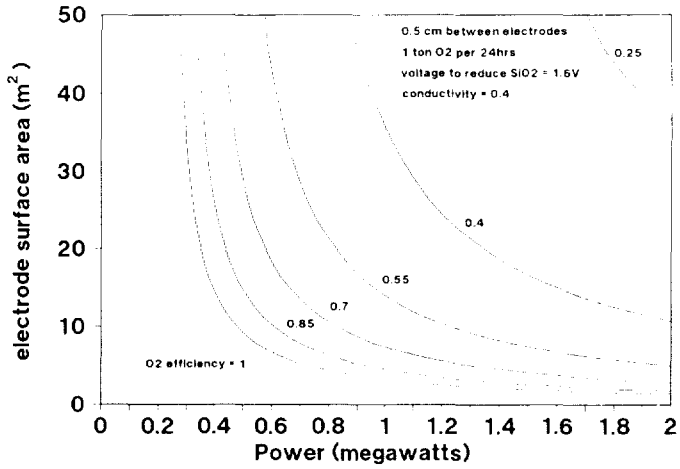

Fig. 12. Effect of electrode surface area and oxygen production efficiency on power required to produce 1 tonne O_2 per 24 hr when the conductivity is 0.4 ohm^{-1}cm^{-2} and the distance between electrodes is 0.5 cm.

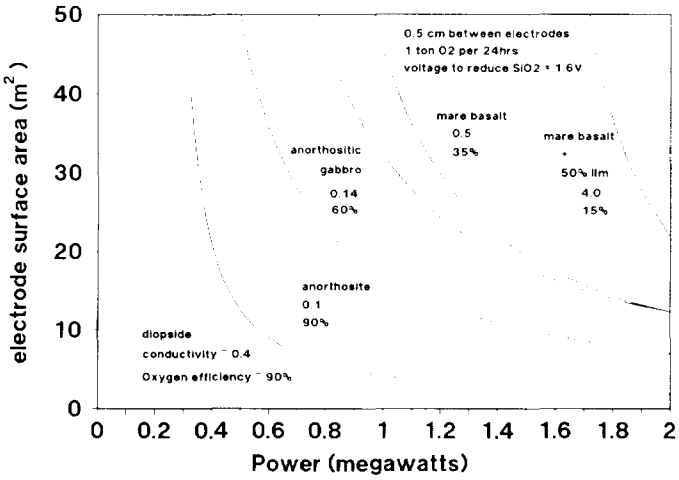

Fig. 13. Power required to produce O_2 at the rate of 1 tonne/24 hr for the conductivities and production efficiencies determined for several real compositions. Power requirements for the high-Fe compositions are high because of the low production efficiencies.

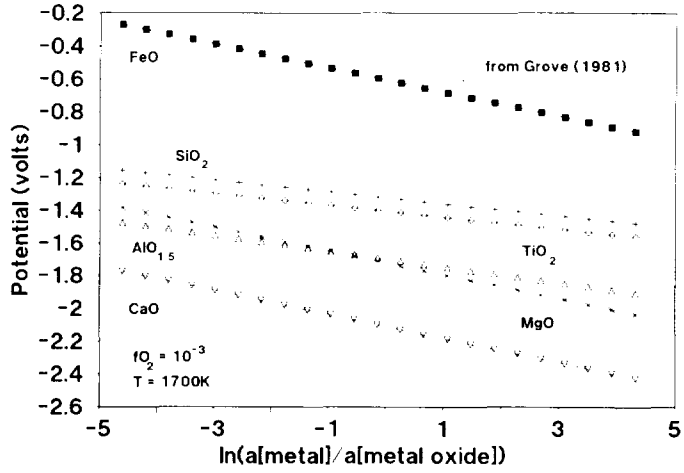

Fig. 14. Relationship between applied potential and equilibrium activities in metal and silicate melt for several oxides at $fO_2 = 10^{-3}$ and temperature = 1700 K. Data are from *Robie and Waldbaum* (1968). The line from *Grove* (1981) is from actual measurements in basaltic melts translated to a standard state in which activity of FeO in the melt is defined as cation mole fraction Fe^{2+} to correspond to the standard state of this study.

Given the data presented in this paper and the thermodynamic data of *Robie and Walkbaum* (1968), presented in Fig. 14, it is possible to follow theoretically the progress of the electrolysis of a single batch of basalt and calculate the power required to produce 1 tonne of O_2. In these calculations we assume ideal solution in the melt and in the metal produced, which introduces some error into the results. However, our own observations of silicate breakdown potential and those of *Grove* (1981) for FeO (e.g., see Fig. 14) demonstrate that for the reduction of Fe^{2+} and Si(IV) any resultant error in the estimates of power consumed will be <20%. The reductions of other species [(Al^{3+}, Mg^{2+}, Ca^{2+}, Ti(IV)] are given for demonstration and may not be numerically exact although they are approximately correct.

In this theoretical electrolysis, we incrementally reduce 0.57 kg of a six-component (SiO_2 = 46.2 wt%, Al_2O_3 = 12.6%, TiO_2 = 2.8%, FeO = 17.4%, MgO = 10.4%, CaO = 10.6%) basaltic melt of a composition similar to Apollo 12 soil (12001; *Laul and Papike,* 1980). At each increment, we recompute the conductivity of the melt (from the relationship in Fig. 3), the production efficiency (from Fig. 8, ignoring contributions from the oxidation of Ti^{3+}), and the equilibrium distribution of components between silicate melt and metal [from the thermodynamic data of *Robie and Waldbaum* (1968) and mass balance constraints, using Newton's method of approximation to solve numerically for the system of 12 nonlinear equations]. The computed variations in conductivity, production efficiency, and remaining amounts of oxides in the silicate melt are shown in Figs. 15 and 16. Although the computations were carried to the point that only CaO remained in the liquid, precipitation of spinel would begin under the conditions of the hypothetical electrolysis (T = 1425°C) at about 35-40 moles oxygen produced.

The potential applied across our imaginary electrolysis cell is

$$E_{applied} = E_C - E_A - \eta_C - \eta_A - i \cdot (R_{cell}) \qquad (14)$$

Here, $E_C - E_A$ is the potential required to reduce the oxides (from which the equilibrium oxide/metal values are calculated), $-\eta_C - \eta_A$ is the overpotential required to drive the reaction at a sufficiently high rate (which we assume is 10% of $E_C - E_A$), i is the current, and R_{cell} is the cell resistance; $R_{cell} = L/(\kappa \cdot A)$, where L is the distance between electrodes, A is the surface area of each electrode, and κ is the melt conductivity. For this exercise, we have chosen L = 0.5 cm and A = 10 m^2 or 30 m^2. The value of $E_C - E_A$ was either increased incrementally from -0.7 to -2 V or was held constant at -1.5 V. The value of pO_2 was held constant at 10^{-3} atm and temperature was 1425°C. The current depends on the constraint that at all times we produce oxygen at the rate

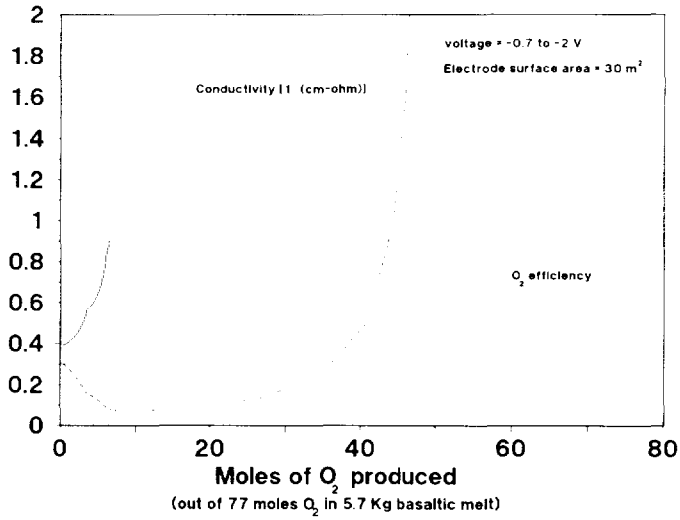

Fig. 15. Moles of O_2 produced as an index of the progress of electrolysis at 1425°C are plotted against conductivity and O_2 production efficiency in accordance with the thought experiment described in the text. This illustrates how these parameters would vary if no interfering process occurred; in fact, at this temperature, spinel is expected to precipitate when 35-40 moles of oxygen have been produced.

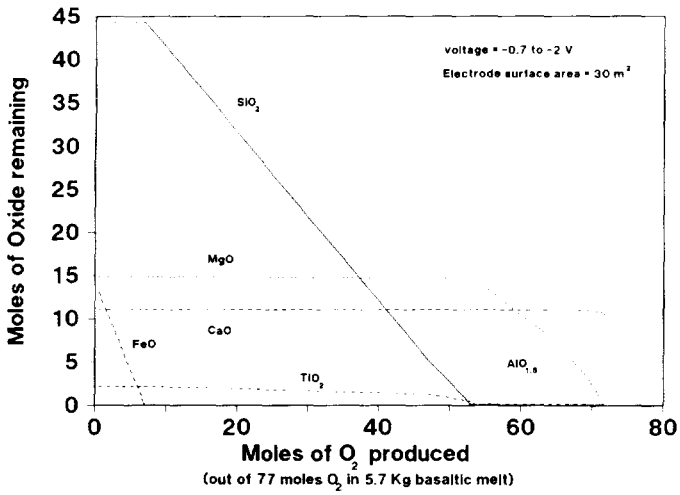

Fig. 16. Moles of oxides remaining (out of 5.7 kg original melt) in the silicate melt during the progress of electrolysis. Same conditions and limitation as in Fig. 15.

of 1 tonne/24 hr (about 140,000 amperes) and on the efficiency of oxygen production, or i (in amperes) = 140,000/O_2 efficiency. The variations of potentials and current during the progress of electrolysis for the case of A = 30 m^2 with E_C - E_A increasing from -0.7 to -2 V are shown in Fig. 17.

Energy requirements per tonne of O_2 as a function of extent of electrolysis are shown in Fig. 18. Energy values for three cases are shown, A = 10 m^2 with potential increasing from -0.7 to -2 V, A = 30 m^2 with potential increasing from -0.7 to -2 V, and A = 30 m^2 with potential constant at -1.5 V. For reduction of one-half of the Si(IV) originally in Apollo 12 soil with an electrode of surface area of 30 m^2 and distance between electrodes = 0.5 cm, the energy required per tonne of O_2 is about 13 MWhr, for an average power requirement of 0.54 MW. Both the conductivity and the production efficiency of the melt improve during the progress of electrolysis; therefore, the extent to which a melt can be electrolyzed depends only on whether the melting point of the residual melt gets too high and, ultimately, on the electrochemical properties of Al^{3+}, Ca^{2+}, and Mg^{2+}, which we have not yet studied. However, based on the phase diagrams of *Osborn et al.* (1954), about half the Si(IV) can be reduced before the liquidus temperature rises above 1425°C and spinel becomes insoluble. If half the original Si(IV) and Ti(IV) is reduced, the amount of Fe^0 produced per 13 MWhr and per 24 hr and per tonne O_2 is about 0.81 tonne, the amount of Si^0 is about 0.65 tonne, the amount of Ti^0 is 0.05 tonne, and the amount of residual silicate melt (with a composition of roughly 40 wt% SiO_2, 2% TiO_2, 22% Al_2O_3, 18% MgO, and 18% CaO) is about 3.5 tonnes.

The feedstock input rate required to derive 1 tonne of O_2 per day under the conditions of the exercise above is about 69 g of feedstock per sec (6.0 tonnes/day). At a density of about 1.5 g/cm^3 for feedstock, this corresponds to some 47 cm^3 of feedstock per sec.

We estimate the energy to convert lunar soil to melt at 1250°-1500°C to be about 480 cal/g, which, at 69 g/sec, corresponds to 0.14 MW. Considering that the reduction requires an additional 0.19 MW, the 0.54 MW (Fig. 18) to operate the cell adds excess resistance heat to the cell at a rate of 0.21 MW. This "waste heat" must be removed from the system.

Actual cell design would take into account that more favorable cell parameters (e.g., larger electrode area or shorter distance between electrodes) or more favorable feedstock conductivity would reduce both the power required and the amount of waste heat. It may be possible to select conditions under which a favorable steady-state composition can be attained for the material in the cell. This composition would lie in the favorable range of conductivity, one corresponding to a substantial reduction in Si(IV) concentration. Such a composition could substantially reduce the excess resistance heating and the corresponding excess power needed.

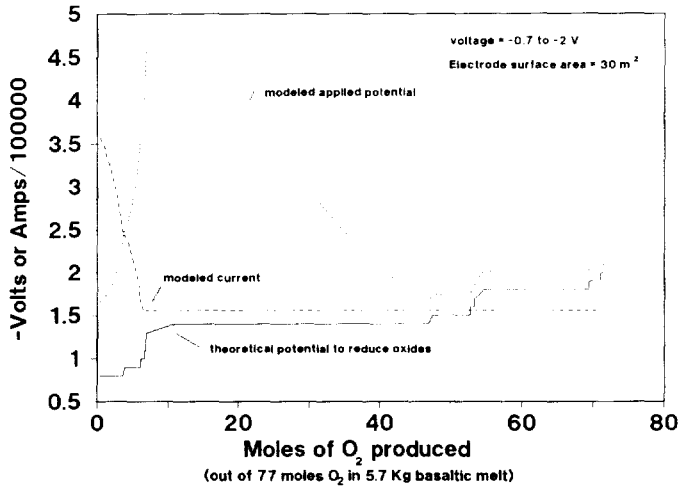

Fig. 17. Variation of imposed potential and current during progress of electrolysis in the thought experiment discussed in the text. By multiplying the maximum voltage by current it is seen that the maximum power requirement is about 0.76 MW. Same conditions and limitation as in Fig. 15.

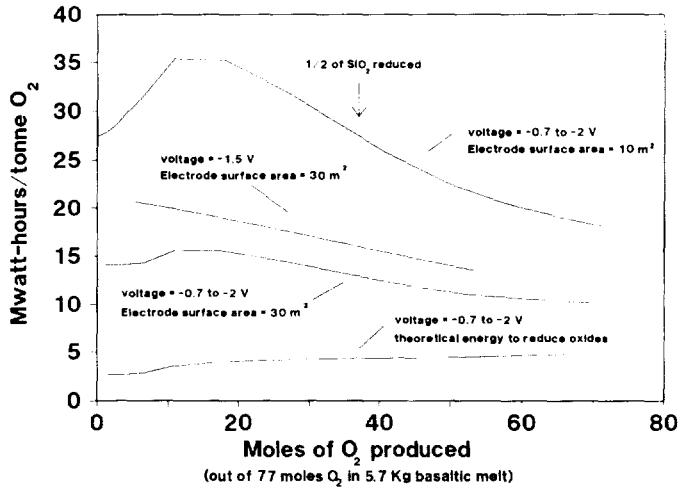

Fig. 18. Energy requirement to produce 1 tonne of O_2 from a basaltic melt of the composition of Apollo 12 soil for the three cases discussed in the text and for the case where no energy is lost to resistance heating, kinetic problems, or low production efficiencies. Same conditions and limitation as in Fig. 15.

In any event, the power going into "waste heat" need not be wasted. Some will be needed to make up for radiation losses from the cell. Depending on conductivities and how the cell is configured, the rest may be regarded as a by-product that can be put to use. For example, both the "waste heat" and the heat contained in the metal and silicate products could be used to heat lunar soil to extract valuable solar-wind implanted gases (H, C, N, and noble gases), or to provide light and heat during the long lunar night. Both the Fe-Si alloy and the residual silicate have to be molten to convert them to useful products. Producing them in the electrochemical cell merely requires that, for efficient use of energy, the appropriate casting forms or drawing or spinning devices handle these materials as they leave the cell.

We have not considered in detail the problems of containers and operations in a cell at high temperature, how to remove and handle the products, or the actual design of an efficient and robust cell. We envision a continuous feed of lunar soil to the cell, and melting of the feedstock by a combination of solar heating and resistance heating. It would seem desirable to have the capability to furnish the entire power for the cell by a source that would not be disrupted by the long lunar nights. The distance between the electrodes could be adjusted during the lunar day to reduce the electrical heating and take advantage of presumably cheaper solar heating (even, perhaps, power) during the lunar days, with the main power coming from a source such as a nuclear reactor, whose share would be increased during the lunar nights.

The apparatus must be housed in a gas-tight container that will capture the oxygen liberated and allow it to be pumped to storage or shipping containers. The dimensions of the housing must be large enough and the materials of the housing refractory enough to be stable in the high-temperature and oxygenating conditions of the cell.

The Si-Fe product can be purified by other techniques to yield Si^0 and Fe^0 or it can be used as ferrosilicon to take advantage of the properties of high-Si iron. These include lower density, corrosion resistance, higher resistivity, lower thermal conductivity, either greater or lesser strength (depending on Si concentration), increased hardness, and reduced ductility. Ferrosilicon can also be used in the manufacture of silicon steels.

Pure Si^0 derived at the cathodes or extracted from the purification of Fe-Si melt can be used in semiconductors (low-volatile conditions on the Moon may make purification of Si easier than it is on Earth), for surfacing mirrors (Si is currently used on Earth for surfacing of dental mirrors), and in photocells. Reoxidation of Si could yield high-purity SiO_2, which could be a source of transparent glass. The residual silicate melt can be used to make beams, rods, tubes, plates, and fibers, which will surely be important if not the dominant constructional materials for use in space. These may have unusually good properties in the water-free space environment, where water will not react with stressed bridging oxygen bonds (e.g., *Blacic*, 1985).

Iron produced by purification of Fe-Si alloys, or by electrolytic precipitation of pure Fe^0 may be used not only as constructional material but for applications we would not consider seriously on Earth, e.g., to surface mirrors (iron will not rust in low lunar pO_2), or as electrical conductors. Copper is very rare on the Moon, and Al is more difficult than Fe to wrest from lunar rock or soil.

The estimates given above demonstrate that the electrochemical properties of lunar silicate melts of themselves do not preclude a practical cell design. Because of the simplicity of the concept and because the power required in this estimate is only about twice the theoretical minimum for separating oxygen from silicate, we anticipate that the process may be quite competitive with others that may be proposed for extracting oxygen from lunar soil or other water-free extraterrestrial silicate materials.

Acknowledgments. We thank C. R. Keedy for his careful review of the manuscript. We appreciate the partial support of this work by the National Science Foundation under grant DAR 79-24705 and by the National Aeronautics and Space Administration under grant NAG 9-56 and through the UA/NASA Space Engineering Center for the Utilization of Local Planetary Resources.

REFERENCES

Arnold J. R. (1979) Ice in the lunar polar regions. *J. Geophys. Res., 84,* 5659-5668.

Blacic J. D. (1985) Mechanical properties of lunar materials under anhydrous, hard vacuum conditions: Applications of lunar glass structural components. In *Lunar Bases and Space Activities of the 21st Century* (W. W. Mendell, ed.), pp. 487-495. Lunar and Planetary Institute, Houston.

du Fresne E. and Schroeder J. E. (1983) Magma electrolysis. In *Research on the Use of Space Resources* (W. F. Carrol, ed.). JPL Publication 83-36.

Greiner E. S., Marsh J. S., and Stoughton B. (1933) *The Alloys of Iron and Silicon.* McGraw-Hill, New York.

Grove T. L. (1981) Use of FePt alloys to eliminate the iron loss problem in 1 atmosphere gas mixing experiments: Theoretical and practical considerations. *Contrib. Mineral. Petrol., 78,* 298-304.

Haskin L. (1992) Water and cheese from the lunar desert. In *The Second Conference on Lunar Bases and Space Activities of the 21st Century,* this volume.

Haskin L. A. and Warren P. (1991) Chemistry. In *Lunar Sourcebook* (G. H. Heiken, D. T. Vaniman, and B. M. French, eds.), pp. 357-474. Cambridge Univ., New York.

Hendersen J., Yand L., and Derge G. (1961) Self-diffusion of aluminum in CaO-SiO_2-Al_2O_3 melts. *Trans. Metall. Soc. AIME, 221,* 56-60.

Henderson P., Nolan J., Cunningham G. C., and Lowry R. K. (1985) Structural controls and mechanisms of diffusion in natural silicate melts. *Contrib. Mineral. Petrol., 89,* 263-272.

Hultgren R., Desai P. D., Hawkins D. T., Gleiser M., and Kelley K. K. (1973) *Selected Values of the Thermodynamic Properties of Binary Alloys, Parts 1 and 2.* American Society for Metals, Metals Park, Ohio. 1435 pp.

Kesterke D. G. (1971) *Electrowinning of Oxygen from Silicate Rocks.* U.S. Bureau of Mines Report of Investigations 7587. 10 pp.

Lanzerotti L. J. and Brown W. L. (1981) Ice in the polar regions of the moon. *J. Geophys. Res., 86,* 3949-3950.

Laul J. C. and Papike J. J. (1980) The lunar regolith: Comparative chemistry of the Apollo sites. *Proc. Lunar Planet. Sci. Conf. 11th,* pp. 1307-1340.

Lewis R. H. (1985) Electrical conductivity measurements of high temperature silicate melts. M.A. thesis, Washington Univ., St. Louis, Missouri. 184 pp.

Lindstrom D. J. and Haskin L. A. (1979) Electrochemical preparation of useful material from ordinary silicate rocks. In *Space Manufacturing Facilities* (J. Grey and C. Krop, eds.), pp. 129-134. American Institute of Aeronautics and Astronautics, New York.

Lindstrom D. J., Haskin L. A., Semkow K. W., and Lewis R. H. (1986) Conductivities of silicate melts: Applications to lunar smelting (abstract). In *Lunar and Planetary Science XVII,* pp. 482-483. Lunar and Planetary Institute, Houston.

Mackenzie J. D. (1962) Oxide melts. *Adv. Inorg. Chem. Radiochem., IV,* 293.

Oppenheim M. J. (1968) On the electrolysis of molten basalt. *Mineral. Mag., 36,* 1104.

Osborn E. F., Devries R. C., Gee K. H., and Kraner H. M. (1954) Optimum composition of blast furnace slag as deduced from liquidus data for the quaternary system CaO-MgO-Al_2O_3-SiO_2. *Trans. AIME, 200,* 33-45.

Pearson G. L. and Bardeen J. (1949) Electrical properties of pure silicon and silicon alloys containing boron and phosphorous. *Phys. Rev., 75,* 865.

Rhodes J. M. and Hubbard N. J. (1973) Chemistry, classification, and petrogenesis of Apollo 15 mare basalts. *Proc. Lunar Sci. Conf. 4th,* pp. 1127-1148.

Rieger P. H. (1987) *Electrochemistry.* Prentice-Hall, Englewood Cliffs, New Jersey. 508 pp.

Rizzo R. A. (1976) Electrochemical studies in calcium magnesium silicate liquids. Ph.D. thesis, Univ. of Wisconsin, Madison. 203 pp.

Robie R. A. and Waldbaum D. R. (1968) *Thermodynamic Properties of Minerals and Related Substances at 298.15°K (25.0°C) and One Atmosphere (1.013 Bars) Pressure and at Higher Temperatures.* U.S. Geol. Surv. Bull. 1259.

Sack R. O., Carmichael I. S. E., Rivers M., and Ghiorso M. S. (1980) Ferric-ferrous equilibria in natural silicate liquids at 1 bar. *Contrib. Mineral. Petrol., 75,* 369-376.

Semkow K. W. and Haskin L. A. (1985) Concentrations and behavior of oxygen and oxide ion in melts of composition $CaO{\cdot}MgO{\cdot}xSiO_2$. *Geochim. Cosmochim. Acta, 49,* 1897-1908.

Semkow K. W. and Haskin L. A. (1986) *Observations on Oxide Film Formation on Platinum Electrodes During Silicate Melt Electrolysis.* McDonnell Center for the Space Sciences Report TEL-108, Washington Univ., St. Louis, Missouri.

Semkow K. W., Rizzo R. A., Haskin L. A., and Lindstrom D. J. (1982) An electrochemical study of Ni^{2+}, Co^{2+}, and Zn^{2+} ions in melts of composition $CaMgSi_2O_6$. *Geochim. Cosmochim. Acta, 46,* 1879-1889.

Simnad M. T., Derge G., and George I. (1954) Ionic nature of liquid iron-silicate slags. *J. Metals, 6,* 1386.

Weast R. C., ed. (1982) *Handbook of Chemistry and Physics,* 63rd edition, p. E-81. CRC Press, Boca Raton.